

**Semi-quantitative immunohistochemical detection of 5-hydroxymethylcytosine reveals conservation of its tissue distribution between amphibians and mammals.**

Rimple D Almeida<sup>1</sup>, Virginie Sottile<sup>1</sup>, Matthew Loose<sup>3</sup>, Paul A De Sousa<sup>2</sup>, Andrew D. Johnson<sup>3</sup> and Alexey Ruzov<sup>1\*</sup>.

**Running title.** 5-hydroxymethylcytosine in amphibian tissues.

**Author affiliations.**

1. Wolfson Centre for Stem Cells, Tissue Engineering and Modelling (STEM), School of Clinical Sciences, Centre for Biomolecular Sciences, University of Nottingham, University Park, Nottingham, NG7 2RD, UK
2. MRC Scottish Centre for Regenerative Medicine, University of Edinburgh, 49 Little France Crescent, Edinburgh EH16 4SB, UK
3. School of Biology, University of Nottingham, University Park, Nottingham, NG7 2RD, UK

\*. To whom correspondence should be addressed. Alexey Ruzov (Email:

[Alexey.Ruzov@nottingham.ac.uk](mailto:Alexey.Ruzov@nottingham.ac.uk), Tel.: +44(0)1158231234).

**Corresponding author:** Alexey Ruzov , Wolfson Centre for Stem Cells, Tissue Engineering and Modelling (STEM), Centre for Biomolecular Sciences, University of Nottingham, University Park, Nottingham, NG7 2RD, UK, Email: [Alexey.Ruzov@nottingham.ac.uk](mailto:Alexey.Ruzov@nottingham.ac.uk), Tel.: +44(0)1158231234.

**Keywords:** epigenetics, 5-hydroxymethylcytosine, 5-methylcytosine, evolution, regeneration, semi-quantitative immunohistochemistry.

**Abstract.**

5-Hydroxymethylcytosine (5-hmC) is a form of modified cytosine, which has recently attracted a considerable attention due to its potential role in transcriptional regulation. According to several reports 5-hydroxymethylcytosine distribution is tissue-specific in mammals. Thus 5-hmC is enriched in embryonic cell populations and in adult neuronal tissue. Here we describe a novel method of semi-quantitative immunohistochemical detection of 5-hmC and utilise it to assess the levels of this modification in amphibian tissues. We show that, similar to mammalian embryos, 5-hmC is enriched in axolotl tadpoles compared to adult tissues. Our data demonstrate that 5-hmC distribution is tissue-specific in amphibians, and that strong 5-hmC enrichment in neuronal cells is conserved between amphibians and mammals. In addition we identify 5-hmC-enriched cell populations which are distributed in amphibian skin and connective tissue in a mosaic manner. Our results illustrate that immunochemistry can be successfully used not only for spatial identification of cells enriched with 5-hmC, but also for the semi-quantitative assessment of the levels of this epigenetic modification in single cells of different tissues.

**Main text.**

5-Hydroxymethylcytosine (5-hmC) is a form of modified cytosine, which has recently attracted a considerable attention due to its potential role in transcriptional regulation and its possible involvement in embryonic stem cells (ESCs) maintenance and differentiation<sup>1,2</sup>. The conversion of 5-mC to 5-hmC is catalysed by *Tet* (Ten-eleven translocation) oncogene family member proteins<sup>3</sup>. According to several recent reports 5-hydroxymethylcytosine distribution is tissue-specific in mammals<sup>3,4,5,6</sup>. Thus 5-hmC is highly enriched in mouse and human embryonic cell populations and in adult neuronal tissue<sup>3,4,5,6</sup>. A number of approaches to 5-hmC detection have been employed. Several of them include a range of biochemical methods based on thin layer chromatography (TLC)<sup>4</sup>, liquid chromatography coupled with mass-spectrometry<sup>6</sup>, capillary

electrophoresis coupled with laser induced fluorescence<sup>7</sup>, enzymatic<sup>8,9</sup> or immunological<sup>10</sup> quantification of 5-hmC levels. These techniques are quantitative but do not supply information concerning the spatial distribution of 5-hmC in different cell types. In contrast, immunocytochemistry and immunohistochemistry provide spatial data, but are not generally considered quantitative.

Here we describe a novel method of semi-quantitative immunohistochemical detection of 5-hmC and utilise it to assess the levels of this modification in a range of amphibian (axolotl, *Ambystoma mexicanum*) tissues. Our data demonstrate that 5-hmC distribution is tissue-specific in amphibians, and that strong 5-hmC enrichment in neuronal cells is conserved between amphibians and mammals. In addition, we identify cell populations containing high levels of 5-hmC which are distributed in amphibian skin and connective tissue in a mosaic manner.

Previously we characterised the 5-hmC distribution in mammalian development employing a standard non-quantitative immunochemical staining procedure based on the use of peroxidase-conjugated secondary antibody coupled with a tyramide signal enhancement system<sup>5</sup>. Using this method we were able to detect 5-hmC in a range of mouse embryonic tissues<sup>5</sup>. Thus immunostaining of 17.5 days post coitum (dpc) mouse embryonic skin reveals a 5-hmC signal in the majority of embryonic epithelial and fibroblast cells (Figure S1A). Since the amount of peroxidase-conjugated secondary antibody in such an immunostaining reaction is expected to be proportional to the amount of primary antibody and ultimately to the amount of antigen (5-hmC) in the specimen, we decided to assess the kinetics of peroxidase reaction with its fluorescent substrate by quantifying the staining intensity on serial adjacent embryonic sections at different times of incubation with tyramide. Assuming that we could detect the rate of peroxidase reaction in its initial linear phase, this would allow us to semi-quantitatively assess the levels of 5-hmC in different specimens, which would be proportional to the velocities of corresponding peroxidase reactions ( $\Delta$  Intensity/  $\Delta$  Time, visually represented by a slope of a reaction progress curve)<sup>11</sup>. At 1:5000

dilution of primary antibody, which we used initially, the progress curve of the reaction became saturated at very short times of incubation with tyramide (Figure S1C, upper panel). In order to detect the linear initial rate period of the reaction's progress curve, we decreased the amount of peroxidase enzyme in the immunostaining by diluting the primary (anti-5-hmC) antibody. We performed the same staining experiment with primary antibody diluted at 1:50 000 and 1:500 000 (Figure S1B, C). Immunostaining with primary antibody at 1:500 000 dilution did not produce detectable signal at any time of incubation (data not shown), but at 1:50 000 primary antibody dilution the progress curve of the reaction was very close to linear (Figure S1C, lower panel). Based on these data we concluded that primary antibody at 1:5000 dilution can be used exclusively for qualitative experiments. By contrast, the progress curve observed using a 1:50 000 dilution of primary antibody suggests that the levels of 5-hmC can be assessed semi-quantitatively at this reduced antibody level. Therefore, to test if we could evaluate the 5-hmC levels in tissues semi-quantitatively using this technique, we carried out the immunostaining of serial adjacent sections of mouse brain and heart, since strong differences in the 5-hmC levels of these organs have been reported by several independent studies<sup>4-8</sup>. Indeed, the progress curves obtained from these tissues were significantly different, with reaction velocities values 0.62 and 0.17 for brain and heart, respectively (Figure S2). These results are in agreement with published data, which show enriched 5-hmC in brain neuronal tissue compared to heart and other adult murine cell types<sup>4,5,7,10</sup>.

The distribution of 5-hmC has been studied only in mammalian tissues to date; therefore whether it plays a conserved function is unknown. Amphibian genomes contain the orthologs of at least two Tet genes, *Tet2* and *Tet3* (Figure 1A) and the transcripts of *Tet3* homolog are expressed at the most of developmental stages as well as in a wide range of adult *Xenopus tropicalis* tissues (Figure 1B). To test if 5-hmC is conserved in vertebrates we decided to look at its distribution in axolotl and *Xenopus*. Evaluating the levels of 5-hmC qualitatively, using 1:5000 dilution of primary antibody, we performed an immunostaining of axolotl tadpole sections and adult tissues

from *Xenopus laevis* and axolotl (*Ambystoma mexicanum*). Similar to mammalian embryos<sup>5</sup> most of axolotl tadpole tissues were strongly enriched in 5-hmC with lower levels of this epigenetic mark in tadpole epithelial cells (Figure 1C-G). High levels of 5-hmC were detected in the neural tissue of *Xenopus* spinal cord but not in intestine, skeletal or heart muscle (Figure 2A). Both axolotl neural tissue (Figure 2B, brain, spinal cord) and skeletal muscle (Figure 2B, muscle) exhibited high levels of 5-hmC. At the same time this modification was undetectable in the overwhelming majority of gut, liver and cartilage cells (Figure 2B, Figure S3 and data not shown). Interestingly, although most of axolotl skin and connective tissue cells did not exhibit any 5-hydroxymethylcytosine signal we identified a population of 5-hmC enriched cells distributed in a mosaic pattern throughout these tissues (Figure 2B, Figure S3). These cells were particularly abundant in gills, the epithelial layer of axolotl skin, and in connective tissue adjacent to the cartilage formations. A similar mosaic distribution of 5-hmC enriched cells was observed in *Xenopus laevis* adult skin (Figure 2A, Figure S4). As expected, 5-methylcytosine was present at equally high levels in all the tested *Xenopus* and axolotl tissues (Figure 2).

Since we detected a strong 5-hmC signal in both axolotl neural tube and skeletal muscle cells, which was different to our results with mammalian tissues<sup>5</sup>, we decided to evaluate 5-hmC levels in these tissues semi-quantitatively. Quantification of our staining results in experiments with 1:50 000 primary antibody dilution revealed that axolotl neural cells were strongly 5-hmC enriched compared to skeletal muscle cells (Figure 3A, Figure S5). Thus 5-hmC signal was detectable in neural tube at the shortest times of incubation with tyramide (10 sec). The neural tube reaction progress curve was significantly different from that of skeletal muscle, however it was similar to the progress curve obtained by quantification of mouse brain staining, with respective reaction velocities of 0.726 and 0.62 (Figure 3A-C, Figure S5). In contrast, progress curves generated from axolotl skeletal muscle and mouse heart contained slopes that were again similar, but much less steep than neural tissue (reaction velocities 0.098 and 0.17, respectively) (Figure 3A-C, Figure S5).

Based on the reaction velocities' calculation we estimate that axolotl neural tissue contains approximately 7 times more 5-hmC than skeletal muscle. Further, experiments with the 1:50 000 antibody dilution showed that reaction velocities indicating relative levels of 5-hmC in axolotl skin (0.398) and connective tissue (0.28) were intermediate between these two groups, (Figure 3A-C), thus these cells also exhibit relatively high 5-hmC content compared to skeletal muscle. However, in the majority of skin and connective tissue cells, we were not able to detect 5-hydroxymethylcytosine using any dilution of anti-5-hmC antibody. To ensure that our staining results were not affected by tissue-embedding procedures we assessed the 5-hmC and 5-mC contents of total DNA extracted from axolotl neural tissue, muscle, cartilage and skin using a dot-blot assay. Whilst 5-mC was present in all the tested axolotl tissues at similar levels, the 5-hmC signal was significantly higher in axolotl neural tissue compared to skin, cartilage and skeletal muscle (Figure 3D). These results agree with our immunohistochemical data, since, according to them, only a proportion of axolotl skin and cartilage cells exhibit high levels of 5-hmC, whereas it cannot be detected in the rest of the cells in these tissues. Thus the quantification of our results show that 5-hmC distribution is tissue-specific in amphibians. Among the tissues tested, axolotl neural tube cells have the highest 5-hmC content, comparable with that of mammalian neuronal cells.

Our data show that tissue specificity of 5-hmC distribution is conserved between amphibians and mammals. Neuronal cells are strongly enriched with 5-hmC compared to the rest of tissues in both groups of vertebrates. At the same time, the presence of 5-hmC-enriched cell populations in amphibian skin and connective tissue represents an important difference in patterns of tissue distribution of this modification between the two vertebrate groups. In conclusion, our results illustrate that immunochemistry can be successfully used not only for spatial identification of cells enriched with 5-hmC, but also for the semi-quantitative assessment of the levels of this epigenetic modification in single cells of different tissues.

### Acknowledgements.

We thank Lorraine Young (STEM, University of Nottingham) for supporting this study and Alexander Kondrashev (University of Nottingham) for help. The authors declare no conflict of interest.

### References.

1. Ito S, D'Alessio AC, Taranova OV, *et al.* Role of Tet proteins in 5mC to 5hmC conversion, ES-cell self-renewal and inner cell mass specification. *Nature* 2010; **7310**:1129-1133.
2. Ficiz G, Branco MR, Seisenberger S, *et al.* Dynamic regulation of 5-hydroxymethylcytosine in mouse ES cells and during differentiation. *Nature*. 2011; **7347**:398-402.
3. Tahiliani M, Koh KP, Shen Y, *et al.* Conversion of 5-methylcytosine to 5-hydroxymethylcytosine in mammalian DNA by MLL partner TET1. *Science* 2009; **324**:930–935.
4. Kriaucionis S, Heintz N. The nuclear DNA base 5-hydroxymethylcytosine is present in Purkinje neurons and the brain. *Science* 2009; **324**:929-930.
5. Ruzov A, Tsenkina Y, Serio A, *et al.* Lineage-specific distribution of high levels of genomic 5-hydroxymethylcytosine in mammalian development. *Cell Res*. 2011 Jul 12. doi: 10.1038/cr.2011.113.
6. Globisch D, Münzel M, Müller M, *et al.* Tissue distribution of 5-hydroxymethylcytosine and search for active demethylation intermediates. *PLoS One* 2010; **12**:e15367.
7. Kraus AM, Park YJ, Plass C, Schmeiser HH. Determination of genomic 5-hydroxymethyl-2'-deoxycytidine in human DNA by capillary electrophoresis with laser induced fluorescence. *Epigenetics*. 2011, **6**:560-565.

8. Szwagierczak A, Bultmann S, Schmidt CS, Spada F, Leonhardt H. Sensitive enzymatic quantification of 5-hydroxymethylcytosine in genomic DNA. *Nucleic Acids Res.* 2010; **38**:19:e181.
9. Song CX, Szulwach KE, Fu Y, *et al.* Selective chemical labeling reveals the genome-wide distribution of 5-hydroxymethylcytosine. *Nat Biotechnol* 2011; **29**:68–72.
10. Li W, Liu M. Distribution of 5-hydroxymethylcytosine in different human tissues. *J Nucleic Acids.* 2011; 2011:870726. Epub 2011 Jun 9.
11. Danson M, Eisenthal R. Enzyme assays: a practical approach. Oxford [Oxfordshire]: Oxford University Press, 2002

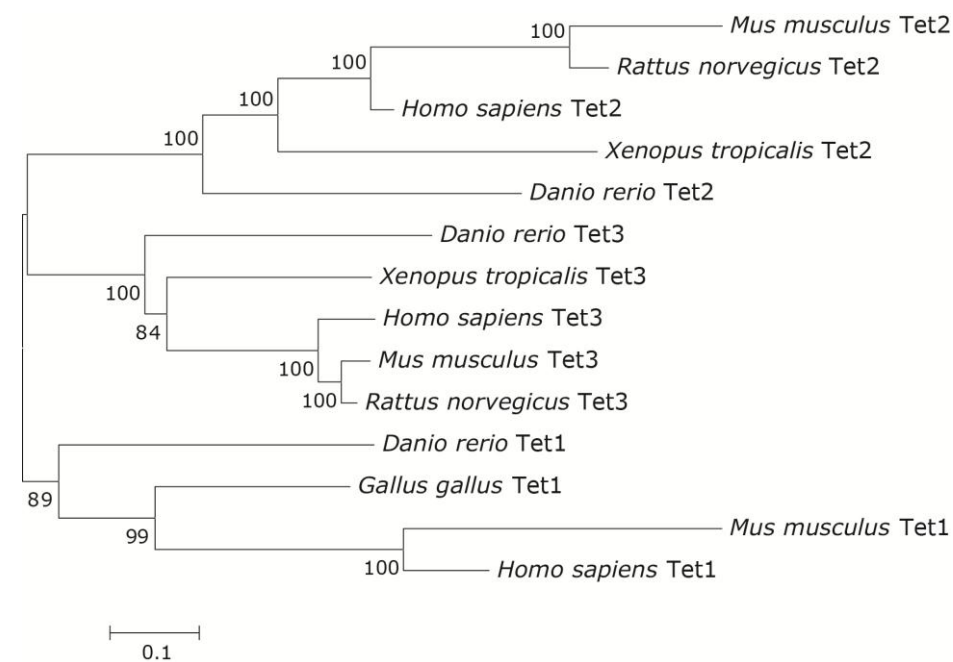
### Figure Legends.

Figure 1. (A) A bootstrap consensus tree inferred using Neighbor-Joining from 100 replicates showing the relationships between *Xenopus*, Zebrafish, Chick, Mouse and Human Tet protein sequences. Although the tree gives the appearance of rooting, it is essentially unrooted. The root is placed at the midpoint of the tree to simplify the presentation. The percentages of replicate trees in which the associated taxa clustered together are shown next to the branches. (B) The developmental stage and tissue distribution of *Xenopus tropicalis* Tet2 and 3 transcripts is determined from NCBI UniGene Est profiles (Tet2:Str.52041 Tet3:Str.53063). Transcript counts are reported in TPM (transcripts per million). (C-G) Immunohistochemical detection of 5-hmC and 5-mC in the tissues of axolotl tadpole. Immunostaining for 5-hmC, 5-mC and merge views are shown. The locations of (D-G) views are indicated with dotted squares on (C).



Figure 2. The distribution of 5-hydroxymethylcytosine in adult *Xenopus* (A) and axolotl (B-C) tissues. 5-hydroxymethylcytosine and 5-methylcytosine have been detected in indicated tissues using 1:5000 dilution of anti-5-hmC antibody. Immunostaining for 5-hmC, 5-mC and merge views are shown. Skel muscle – skeletal muscle. Scale bars are 20  $\mu$ m.

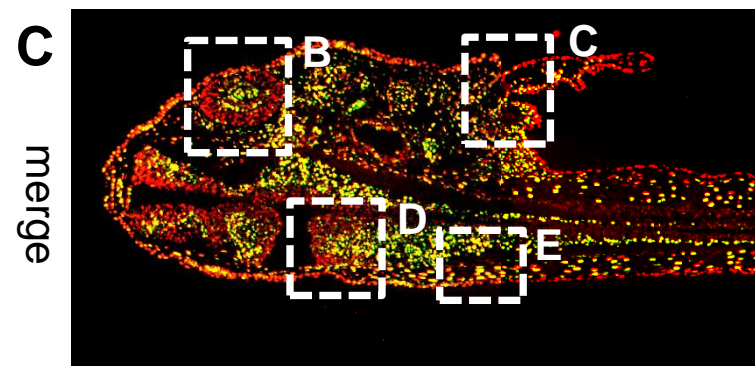
Figure 3. . The semi-quantitative assessment of 5-hmC distribution in adult axolotl tissues. (A) 5-hmC immunostaining signal using 1:50000 dilution of primary antibody at indicated times of incubation with tyramide on sections of axolotl spinal cord (neural tube, N tube), skeletal muscle (Muscle), skin and connective tissue adjacent to cartilage (Cartl). Adjacent sections were stained in parallel at identical conditions with different times of incubation with tyramide. The exposures are identical for all the presented pictures. Examples of regions, which were used for signal quantification, are shown with yellow-line shapes. (B) The progress curves of peroxidase reactions produced by quantification of immunostaining data for different axolotl and mouse tissues. “Skin” and “Cartilage” refers to 5-hmC enriched cells found in these tissues. Most of skin and cartilage cells do not exhibit any detectable staining at any times of incubation with tyramide (A). (C) The velocities of peroxidase reactions for different axolotl and mouse tissues (indicated). (D) The quantification of the dot-blot results performed with a total DNA derived from the indicated axolotl tissues using anti-5-hmC (5-hmC) and anti-5-mC (5-mC) antibodies. The graphs show the dependence of the dot-blot signal intensity of different concentrations of total DNA (indicated).

**A****B**

Stage	xtTet2	xtTet3
Egg	0	0
Gastrula	0	49
Neurula	12	85
Tailbud	0	48
Tadpole	0	19
Adult	0	15

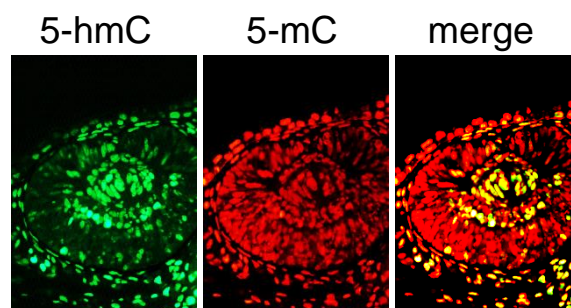
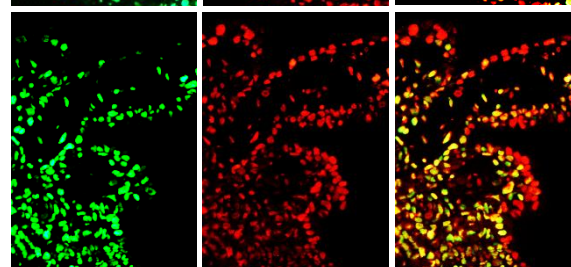
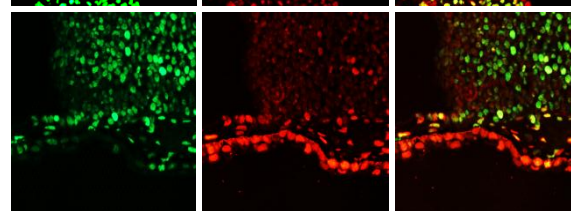
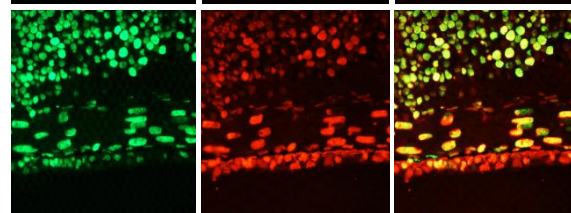
Tissue	xtTet2	xtTet3
Brain	0	50
Head	0	29
Spleen	0	59
Testis	0	23

**C**

merge

5-hmC

5-mC

**D****E****F****G**

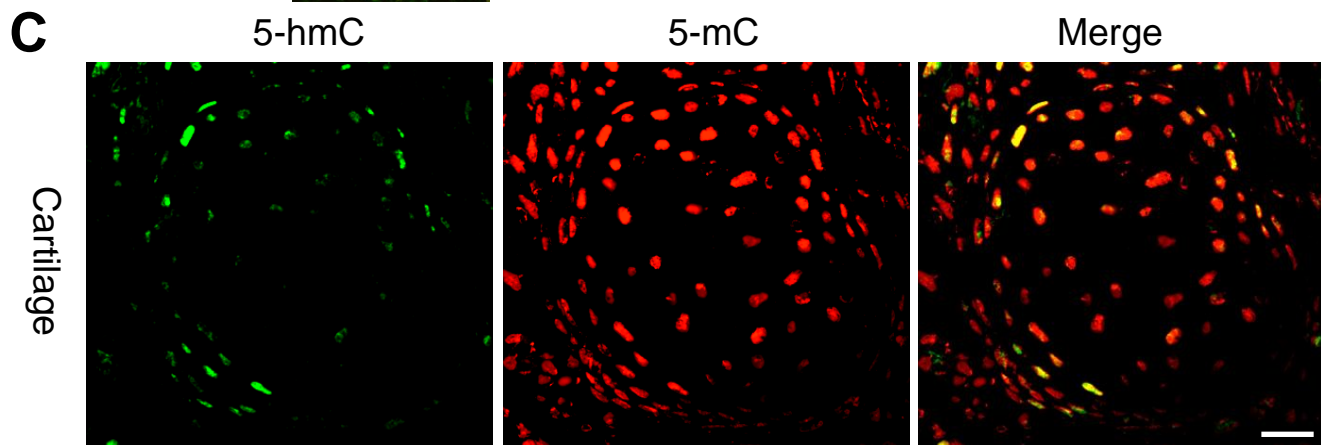
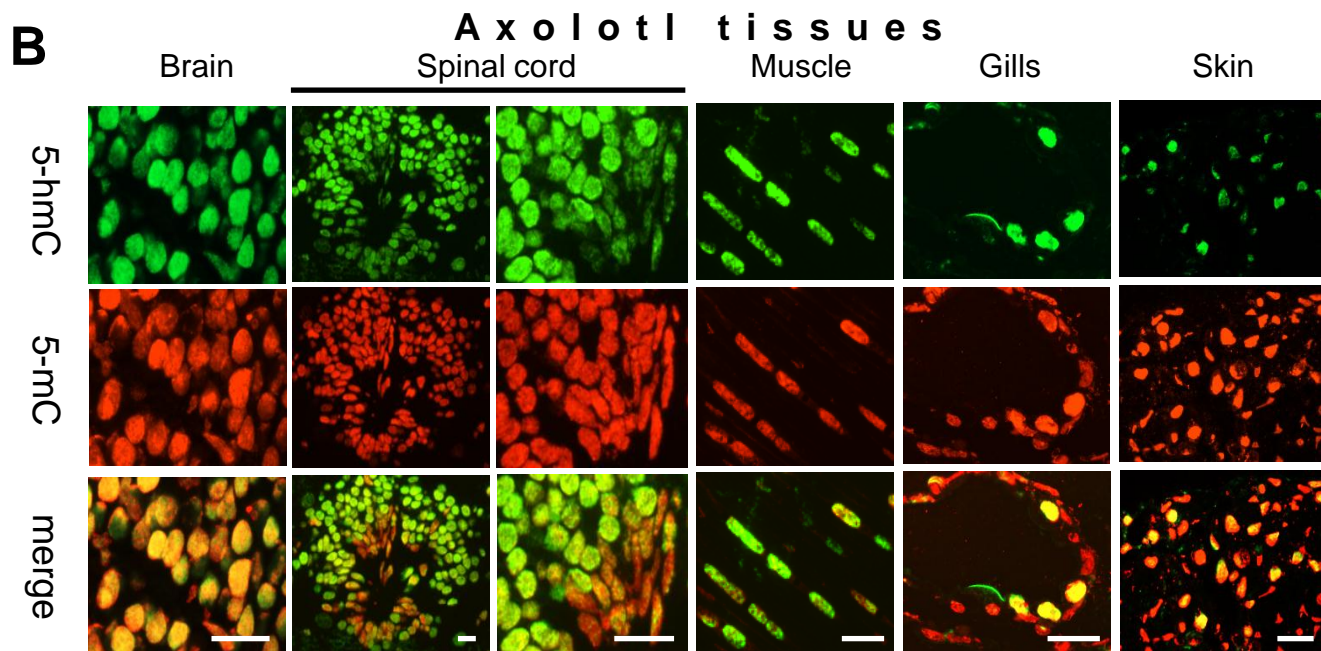
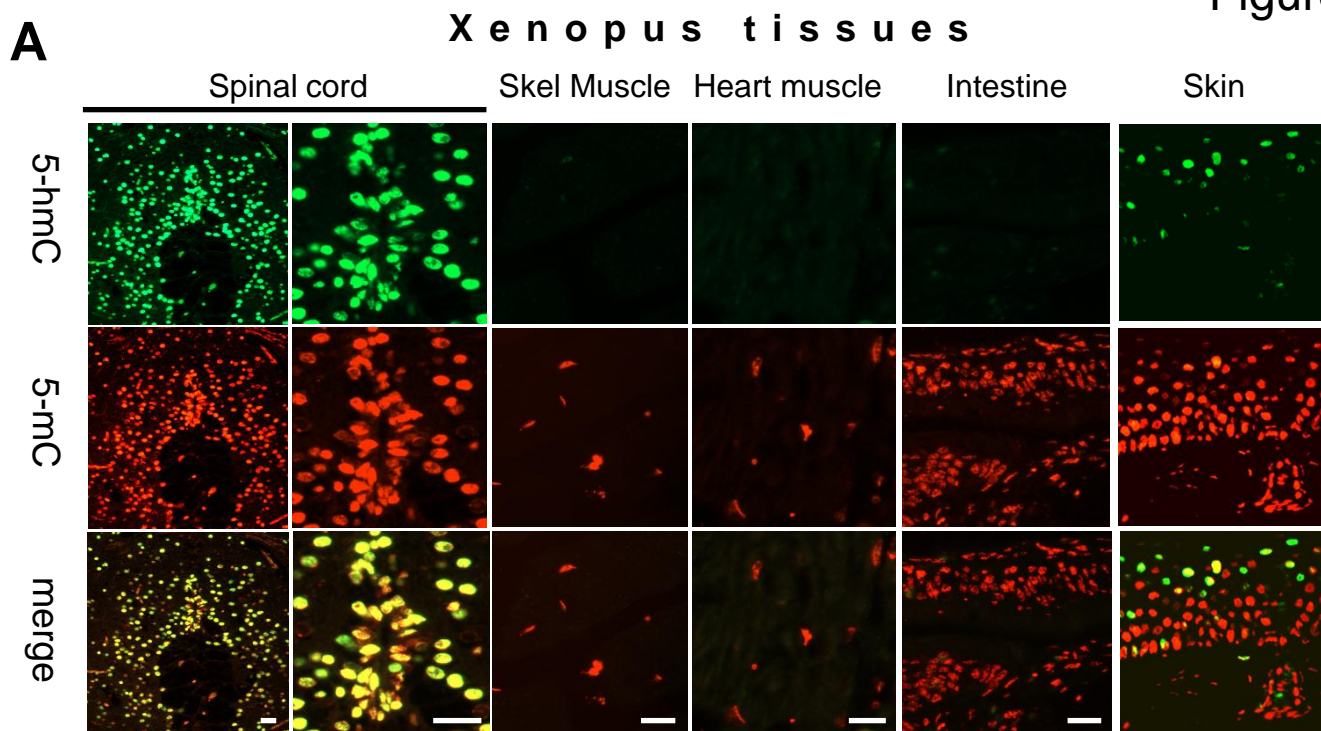
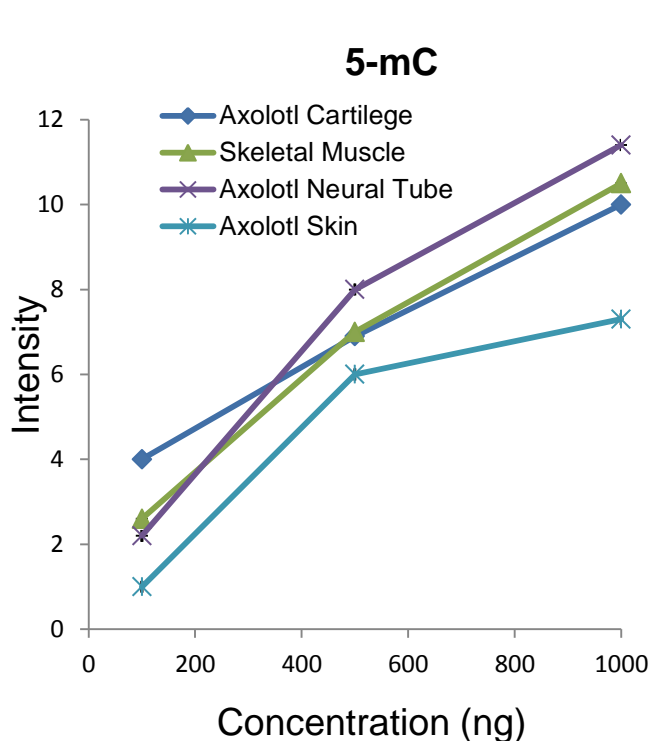
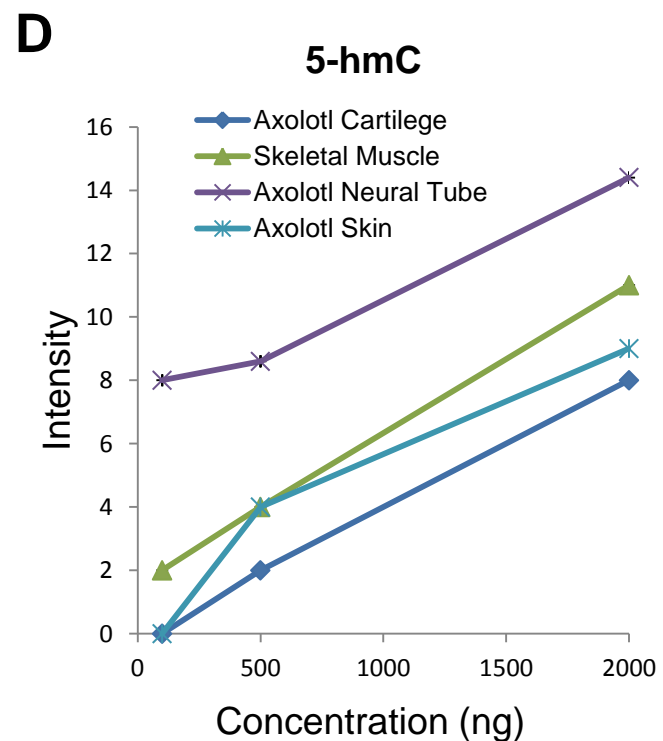
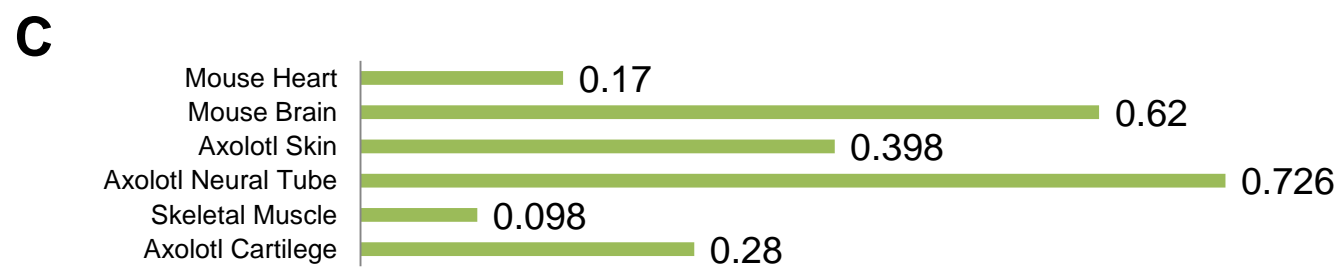
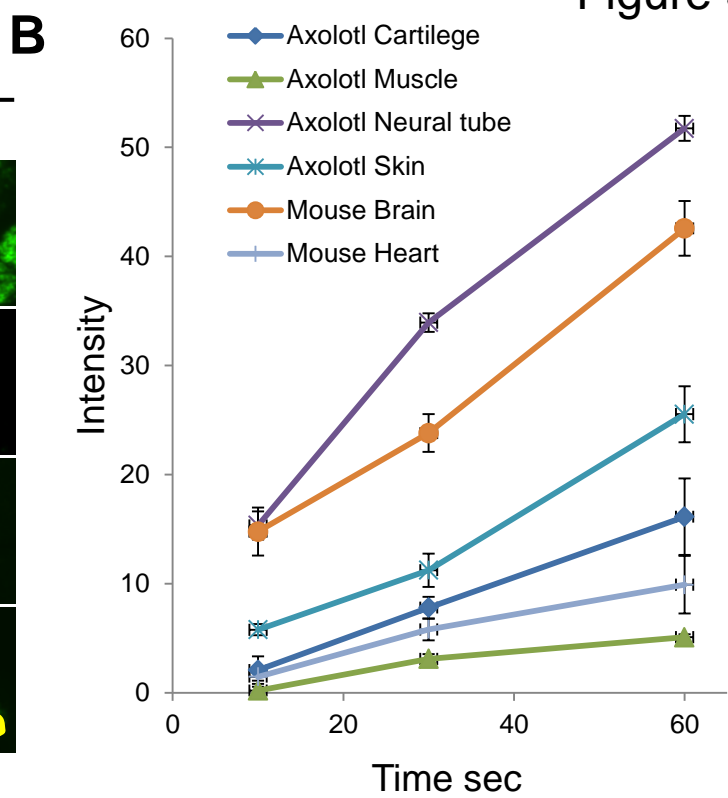
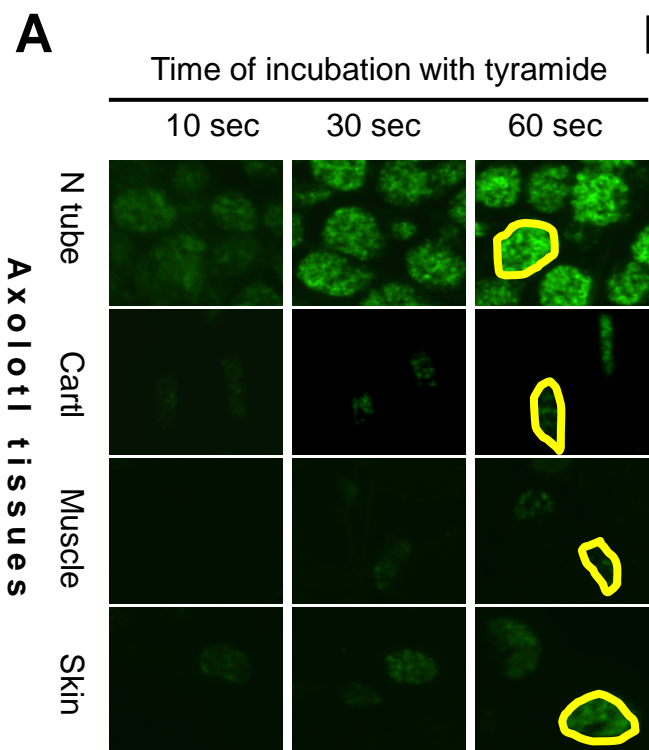
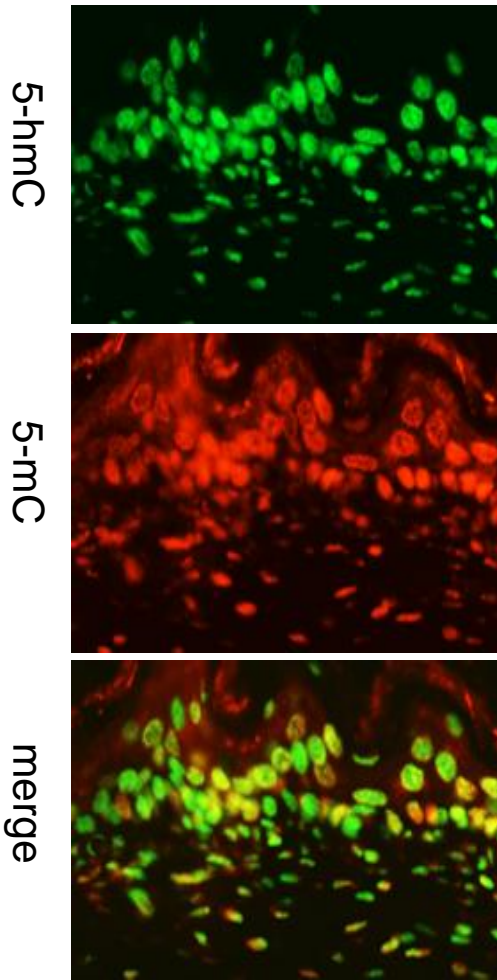


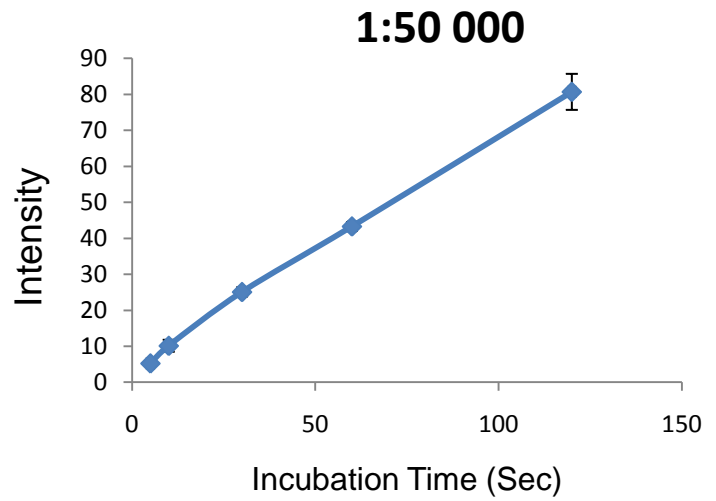
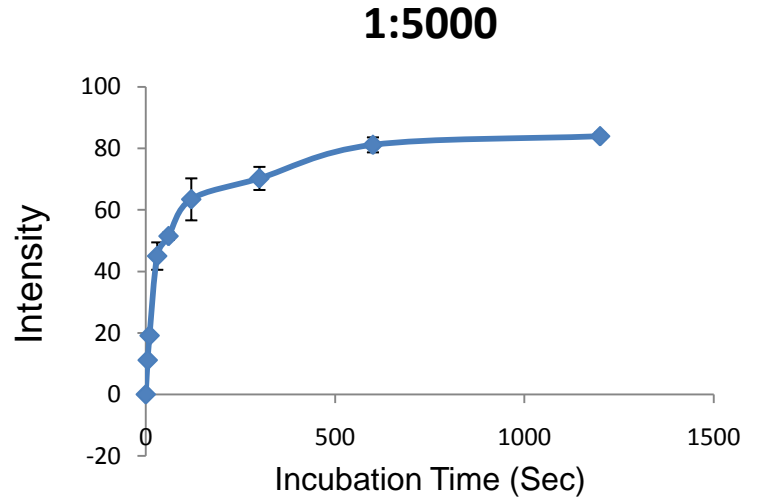
Figure 3



A



C



B

Time of incubation with tyramide

5 sec

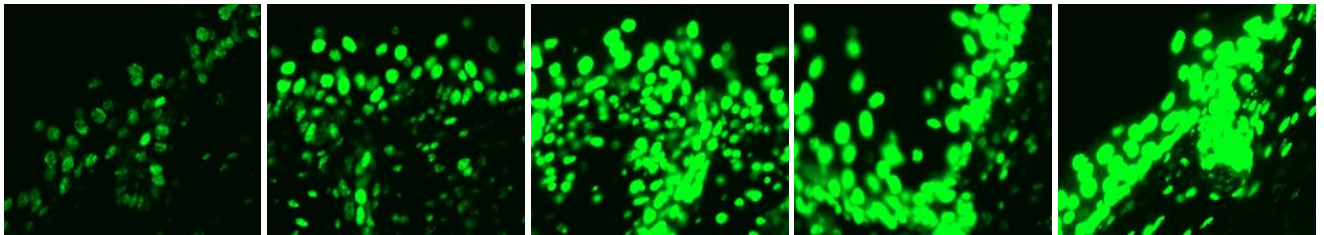
10 sec

30 sec

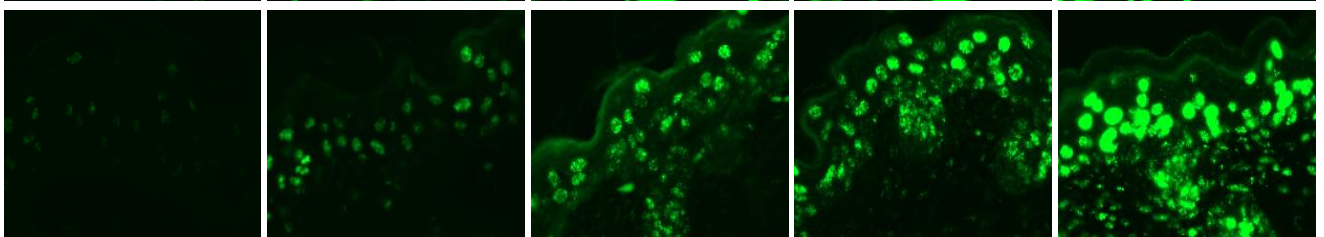
60 sec

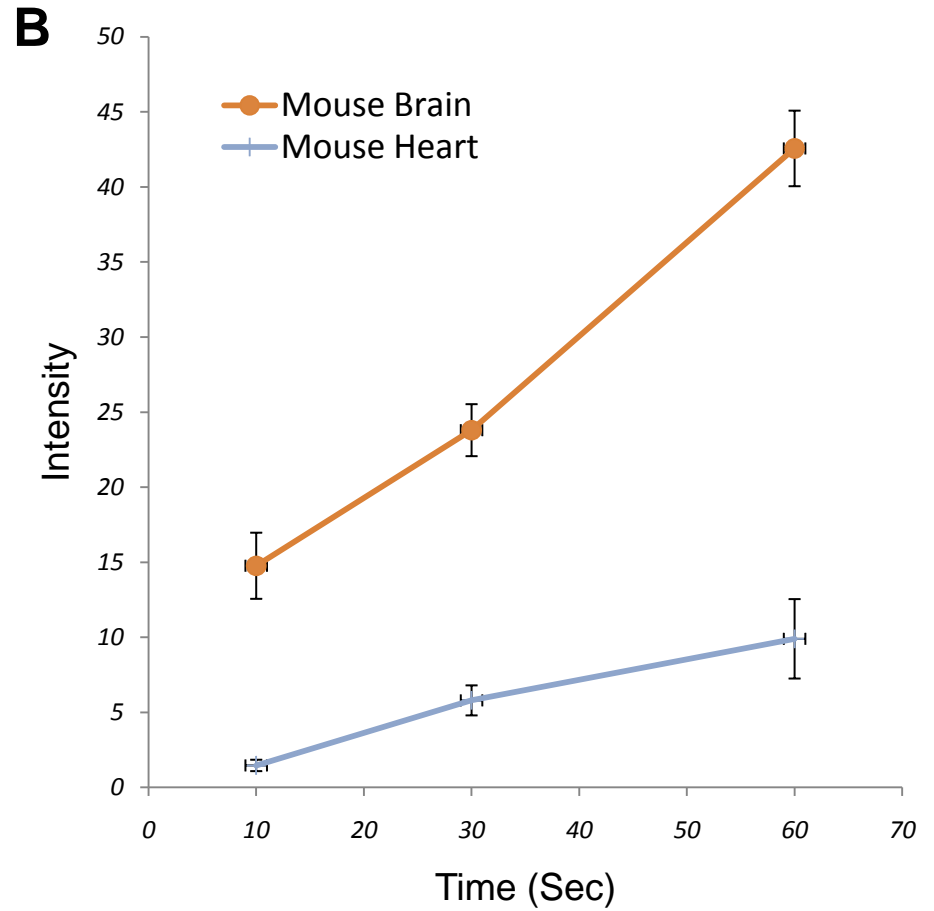
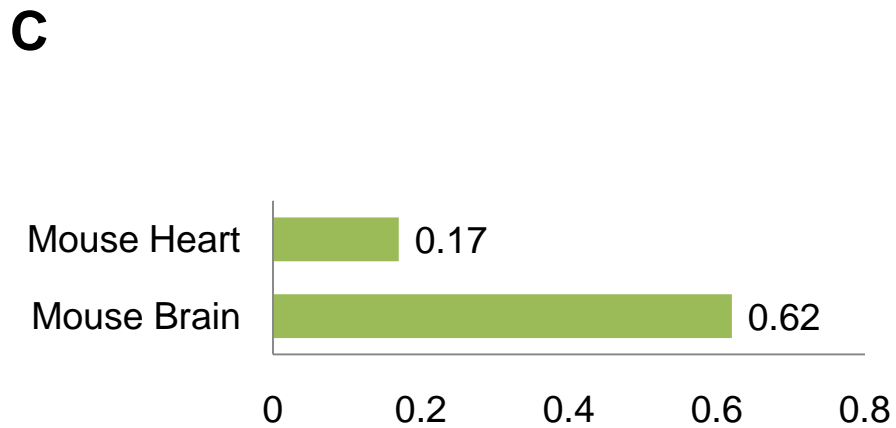
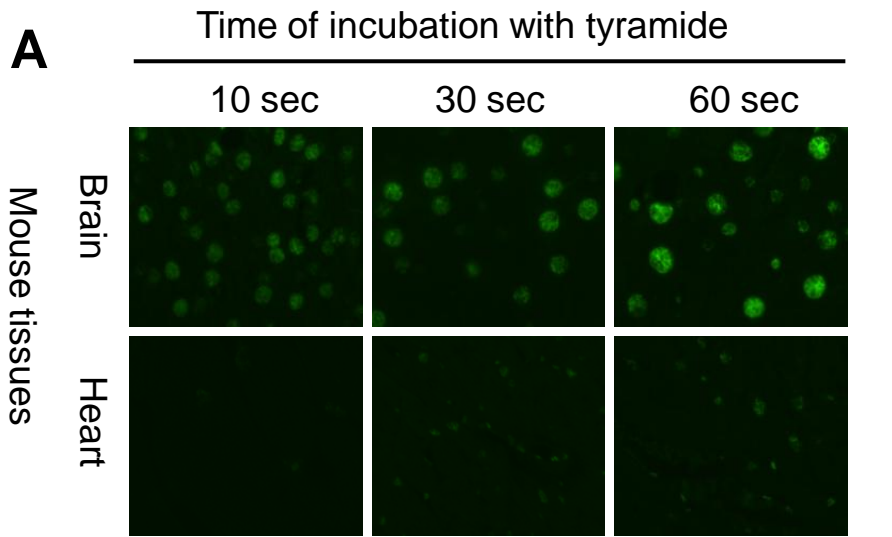
120 sec

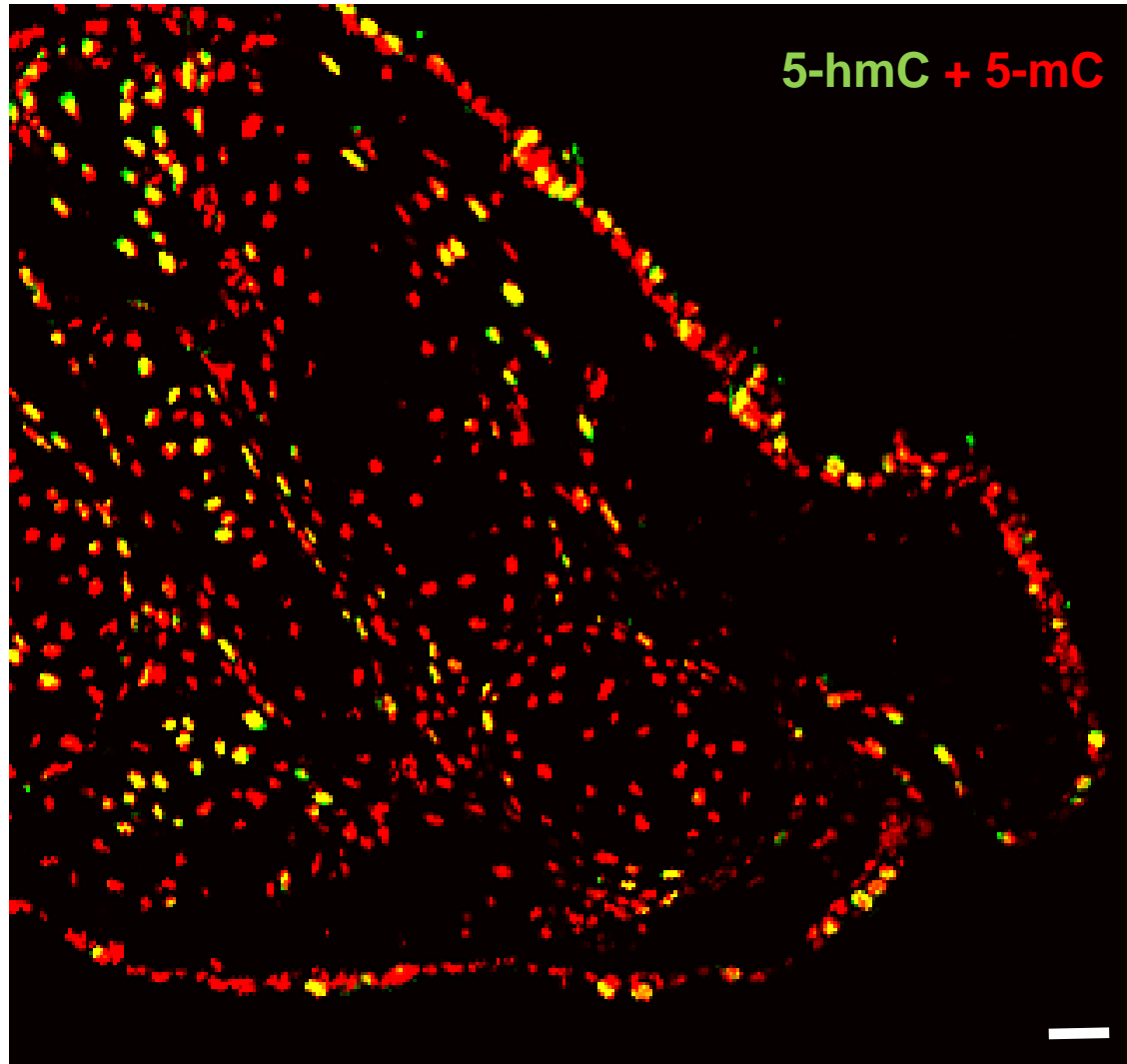
1:5000



1:50 000

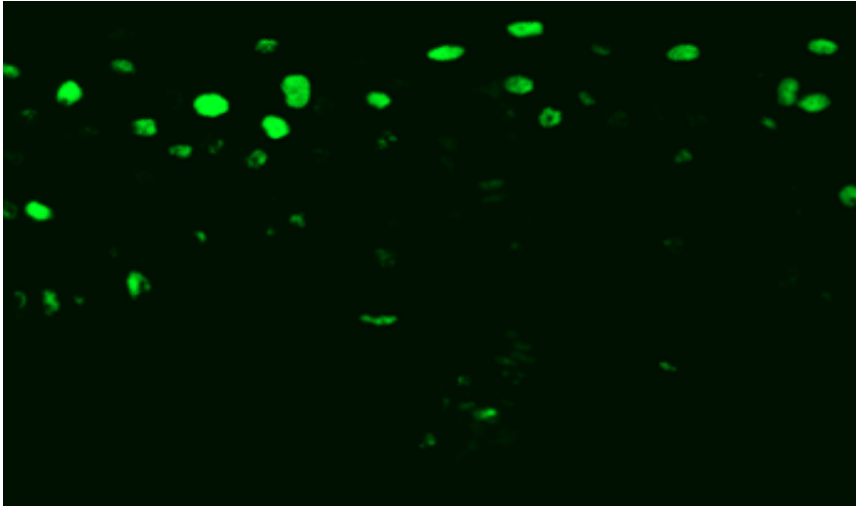




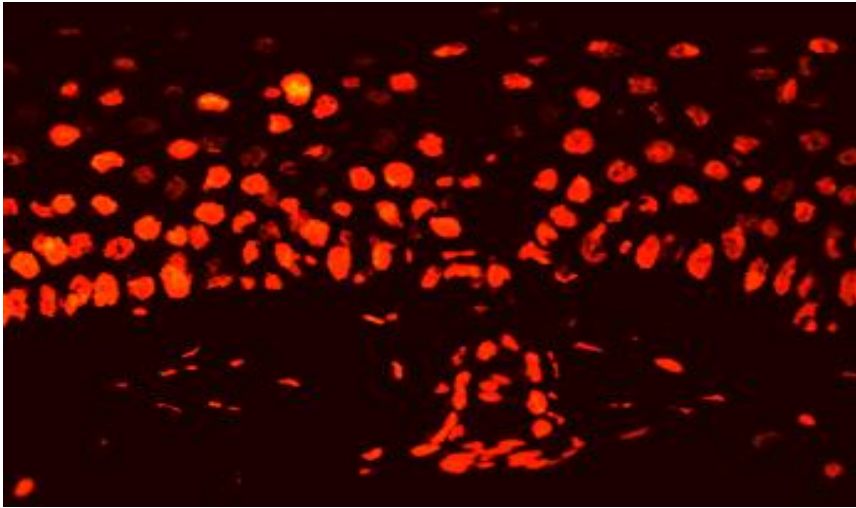


*Xenopus leavis* skin

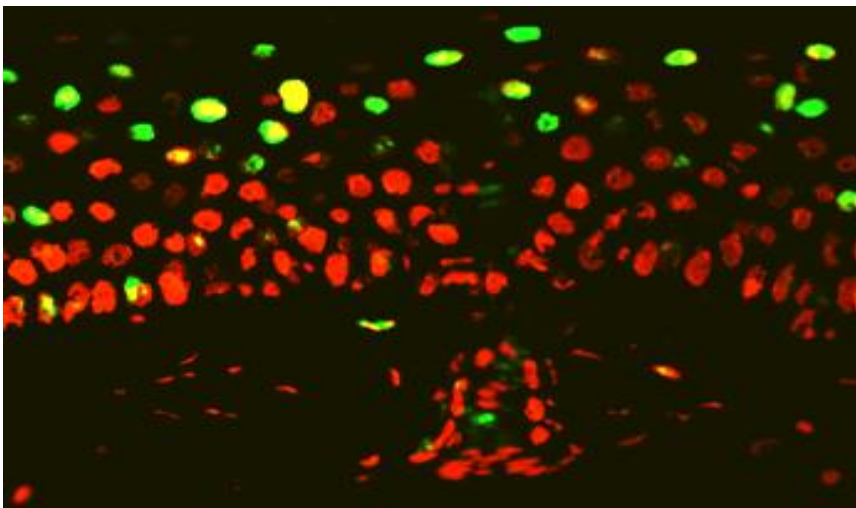
5-hmC



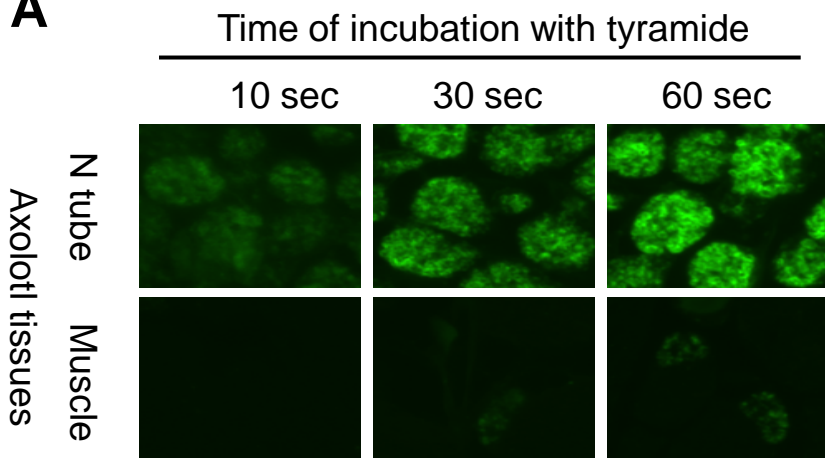
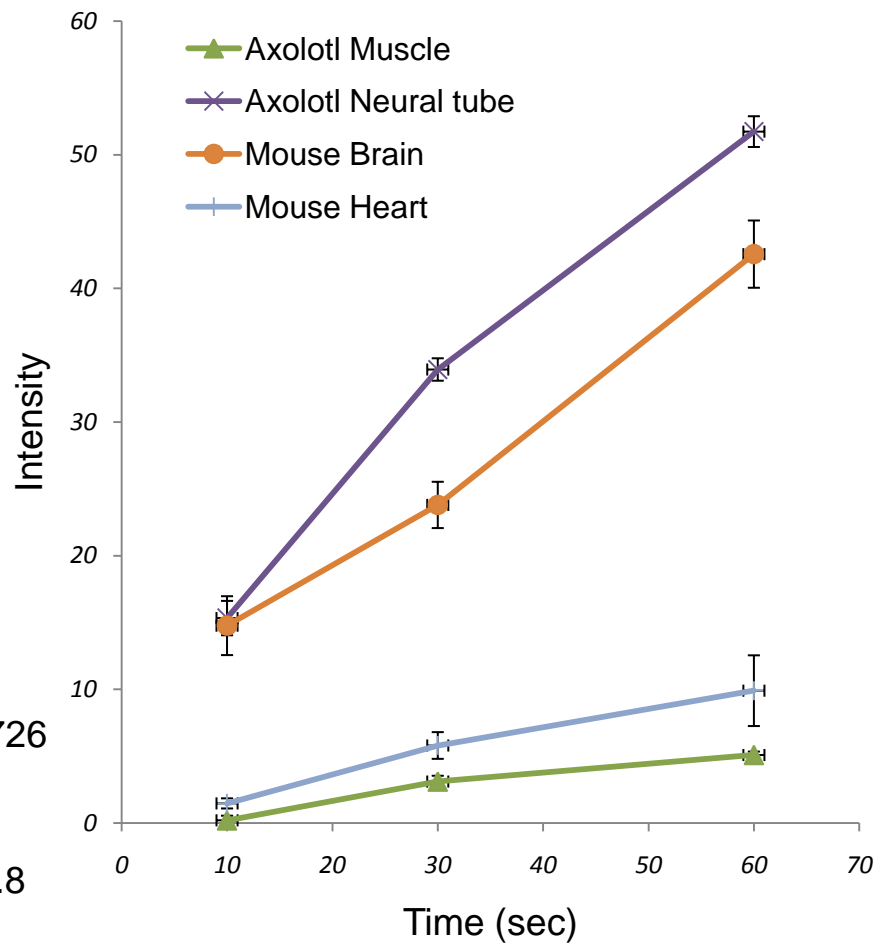
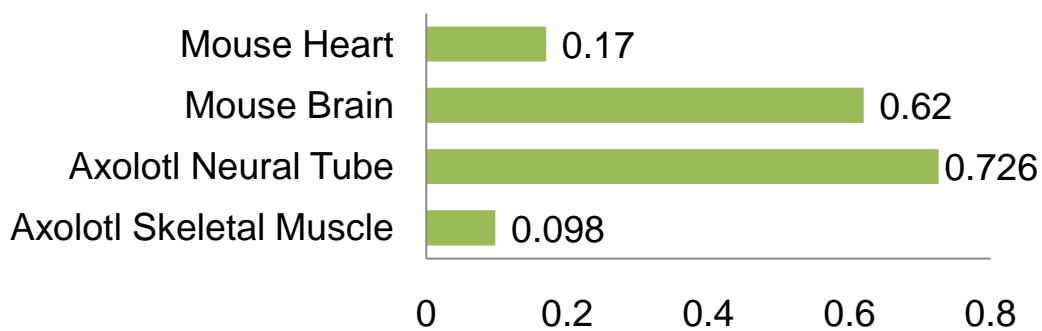
5-mC



merge





**A****B****C**

## **Supplementary information.**

### **Materials and methods.**

**Immunohistochemistry and imaging.** Paraffin embedded formaldehyde fixed sections of axolotls, *Xenopus laevis*, wild type CD1 mouse embryonic and adult tissues were used for immunohistochemistry. Tissues were fixed in 4% formaldehyde for 12 hours. Tissue sections were de-waxed according to standard procedures and permeabilised for 15 min with PBS containing 0.5% Triton X-100. For 5-hmC and 5-mC staining, permeabilised tissue sections were incubated in 4N HCl for 1h at 37°C and then neutralised in 100 mM Tris-HCl (pH 8.5) for 10 min, followed by a standard immunostaining protocol. Anti-5-hmC (Active Motif, 1:5000; 1:50000 and 1:500 000 dilutions) and anti-5-mC (Eurogentec) primary antibodies were used. Peroxidase-conjugated anti-rabbit secondary antibody (Dako) and the tyramide signal enhancement system (Perkin Elmer) were employed for 5-hmC detection. 5-mC was visualised using 555-conjugated secondary antibody (Alexafluor). Control staining without primary antibody produced no detectable signal. Images were acquired using a Nikon ECLIPSE 90i immunofluorescence microscope and Volocity software.

**Image quantification** was performed using Fiji software. Slides with serial adjacent sections were processed under identical conditions with varying times of incubation with tyramide and were imaged at the same exposure settings. Mean intensities were measured for 10-20 random cell nuclei on each region of interest for each sample (examples of measured regions are presented in Figure 1D). Mean values of the mean intensities were plotted onto graphs. Experimental error is expressed as s.e.m. Reaction velocities were calculated as  $\Delta$  Intensity/  $\Delta$  Time, with  $\Delta$  as a difference between experimental points with minimal and maximal times of incubation with a fluorescent enhancer.

**Dot blot assays** were performed as reported previously<sup>1</sup> using anti-5-hmC (Active Motif, 1:5000 dilution) and anti-5-mC (Eurogentec, 1:1000 dilution) primary antibodies. Equal dilutions of axolotl tissues derived DNA were loaded onto membrane. The dilution rate between two neighbouring experimental points equalled 10X. Image quantification was performed using Fiji software. Mean

intensities for different concentrations of genomic DNA were plotted onto graphs. Principally identical results were produced using anti-5-hmC antibody produced by Diagenode.

**Bioinformatic analysis.** The 14 Tet1/2/3 sequences from different species were aligned using RevTrans<sup>1</sup> and all positions containing gaps and missing data were removed. There were a total of 1518 positions in the final dataset. Evolutionary analyses were conducted in MEGA5<sup>2</sup>. NCBI Accession numbers for the sequences used are Homo sapiens Tet1:NM\_030625, Tet2:NM\_001127208, Tet3:NM\_144993 Mus musculus Tet1:NM\_027384, Tet2:NM\_001040400, Tet3:NM\_183138 Rattus norvegicus Tet2:XM\_227694, Tet3:XM\_001057850 Xenopus tropicalis Tet2:XM:002934777, Tet3:NM\_001097187 Gallus gallus Tet1:XM\_421571. Danio rerio sequences were identified from Ensembl (version Zv9 of the Zebrafish genome) as Tet1:ENSDARG00000075230, Tet2:ENSDARG00000076928, Tet3:ENSDARG00000062646. The developmental stage and tissue distribution of Xenopus tropicalis Tet 2 and 3 transcripts is determined from NCBI UniGene Est profiles (Tet2:Str.52041 Tet3:Str.53063). Transcript counts are reported in TPM (transcripts per million).

### **Supplementary Figures legends.**

**Figure S1.** (A) The distribution of 5-hydroxymethylcytosine (5-hmC) and 5-methylcytosine (5-mC) in embryonic skin of 17.5 dpc mouse embryo. 5-hmC, 5-mC staining and merge views are shown. Immunostaining was performed with 1:5000 dilution of a primary anti-5-hmC antibody. (B) 5-hmC immunostaining signal at indicated times of incubation with tyramide in serial adjacent sections of mouse embryonic skin. The primary anti-5-hmC antibody dilutions used (1:50000, and 1:500000) are indicated. Sections were stained in parallel under identical conditions with different times of incubation with tyramide. The exposures are identical for all the presented pictures. (C) The progress curves of peroxidase reactions produced by quantification of immunostaining data presented in (C) with indicated dilutions of an anti-5-hmC antibody.

**Figure S2.** (A) 5-hmC immunostaining signal at indicated times of incubation with tyramide in serial adjacent sections of mouse adult brain and heart. The primary anti-5-hmC antibody was used at 1:50000 dilution. Sections were stained in parallel under identical conditions with different times of incubation with tyramide. The exposures are identical for all the presented pictures. (B) The progress curves of peroxidase reactions produced by quantification of immunostaining data presented in (A) for mouse brain and heart (indicated). (C) The velocities of peroxidase reactions for mouse brain and heart immunostaining experiments.

**Figure S3.** The mosaic distribution of 5-hydroxymethylcytosine in axolotl skin and connective tissue. 5-hmC was visualised using green tyramide on a lateral section through the head region of young axolotl adult. 5-mC staining is shown in red. Merged view is presented. Cells strongly enriched with 5-hmC appear green or yellow on a merged view.

**Figure S4.** The mosaic distribution of 5-hydroxymethylcytosine in the skin of adult clawed frog *Xenopus laevis*. 5-hmC, 5-mC staining and merged views are shown.

**Figure S5.** (A) 5-hmC immunostaining signal at indicated times of incubation with tyramide in serial adjacent sections of axolotl neural tube and skeletal muscle. The primary anti-5-hmC antibody was used at 1:50000 dilution. Sections were stained in parallel in identical conditions with different times of incubation with tyramide. The exposures are identical for all the presented pictures. (B) The progress curves of peroxidase reactions produced by quantification of immunostaining data presented in (A) together with the progress curves obtained for mouse brain and heart staining experiments. (C) The velocities of peroxidase reactions for axolotl brain and skeletal muscle in comparison to those of mouse brain and heart.

**Supplementary references.**

1. Nestor, C., Ruzov, A., Meehan, R., Dunican, D. Enzymatic approaches and bisulphite sequencing cannot distinguish between 5-methylcytosine and 5-hydroxymethylcytosine in DNA. *Biotechniques* 2010; **48**: 317-319.
2. Wernersson R and Pedersen AG. RevTrans - Constructing alignments of coding DNA from aligned amino acid sequences. *Nucl. Acids Res.* 2003; **31**:3537-3539.
3. Tamura K., Dudley J., Nei M., and Kumar S. MEGA4: Molecular Evolutionary Genetics Analysis (MEGA) software version 4.0. *Molecular Biology and Evolution* 2007; **24**:1596-1599.